Noname manuscript No.
(will be inserted by the editor)

Flow interaction between a streamwise oscillating cylinder and a downstream stationary cylinder

S. J. Xu · L. Gan · Y. Zhou

Received: date / Accepted: date

Abstract In this paper we present some experimental results about the physical effects of a cylinder's streamwise oscillation motion on a downstream one in a tandem arrangement. The upstream cylinder undergoes a controlled simple harmonic oscillation at amplitudes $A/d = 0.2 \sim 0.8$, where d is the cylinder diameter, and the frequency ratio of $f_e/f_s = 0 \sim 3.0$, where f_e is the cylinder oscillation frequency and f_s is the natural frequency of vortex shedding from a single stationary cylinder. Under these conditions, the vortex shedding is locked to the controlled oscillation motion. Flow visualization using the planar laser-induced fluorescence (LIF) and qualitative measurements using hot-wire anemometry (HWA) reveal three distinct flow regimes behind the downstream cylinder. For $f_e/f_s > (f_e/f_s)_c$, where $(f_e/f_s)_c$ is a critical frequency ratio which depends on A/d and Reynolds number Re, a so called SA-mode occurs. The upstream oscillating cylinder generates binary vortices symmetrically arranged about the centreline, each containing a pair of counter-rotating vortices, and the downstream cylinder sheds vortices alternately at $0.5f_e$. For $0.7 \sim 1.0 < f_e/f_s < (f_e/f_s)_c$ a complex vortex street that consists of two outer rows of vortices generated by the oscillating cylinder and two inner rows of vortices shed from the downstream stationary cylinder, which is referred to as AA-mode. For $0.3 \sim 0.6 < f_e/f_s < 0.8 \sim 1.0$, one single staggered vortex street (A-mode) is observed. It also is found that, when f_e/f_s is near unity, the streamwise interaction of the two cylinders gives rise to the most energetic wake in the corss-stream direction, in terms of its maximum width, and the wake is AA-mode like. The effects of other parameters such as the spacing between the two cylinders, Re and A/d on the flow pattern are also discussed in details. The observations are further compared to the stationary tandem cylinder cases.

Keywords vortex shedding, tandem cylinders, forced streamwise oscillation, LIF, HWA

S. J. Xu
School of Aerospace Engineering
Tsinghua University, 100084, China
E-mail: xu_shengjin@tsinghua.edu.cn

L. Gan
School of Engineering and Computing Sciences
Durham University, DH1 3LE, UK

Y. Zhou
Shenzhen Graduate School
Harbin Institute of Technology, 518000, China

1 Introduction

Flow behind multiple structures in a cross flow is frequently seen in engineering applications. When the Reynolds number Re, exceeds a critical value, boundary layer separates, forming the well-known Karman vortex street. The alternative vortex shedding from the structure in turn induces structural vibrations at a significant magnitude sometimes (Blevins, 1994). Such vibrations further influence the flow and subsequently the loadings on the downstream structures. From a different perspective, the effect of a controlled oscillating cylinder on the downstream cylinder's wake is important for flow-control applications, where the unsteady flow pattern can be altered or cancelled, which may be used to suppress flow-induced vibrations, or to reinforce them for enhancing fluid mixing. For instance, Karniadakis & Triantafyllou (1989) placed an oscillating cylinder upstream of another cylinder to control the vibration of

the latter; Ming & Gu (2005) showed that a tiny perturbation generated by an oscillating strake on the nose tip of an aircraft may significantly reduce and even eliminate the side force at large angles of attack; acousticians frequently come across a problem to identify the vortex-sound source in a complicated dynamic system such as an aircraft (Hardin & Wang, 2003), which may involve oscillating slender structures. The knowledge of such interactions between the flow generated by an oscillating structure and its neighbouring structures could be important for the identification of the vortex-sound source and to further understand the physics associated with the vortex-sound wave (Inoue & Hatakeyama, 2002). It is therefore of both fundamental and practical interests to investigate how an oscillating cylinder interacts its neighbouring cylinders.

Previous studies mostly focused on the transverse oscillation of one or both cylinders (Williamson & Roshko, 1988; Staubli & Rockwell, 1989; Hover *et al*, 1998; Carberry *et al*, 2001; Zhou *et al*, 2001; Xu & Zhou, 2003, among others). Sumner (2010) reviewed the multiple structure problem in a two-cylinder system, which involves side-by-side, in-tandem or staggered arrangements. Chen (1987) showed that when a lightly damped cylindrical structure is immersed in a liquid, the problem of streamwise vibration could be particularly severe. Structural failure may result from resonance effect between the fluid excitation force and the system natural frequency.

There have been a number of experimental investigations involving a single cylinder oscillating in the streamwise direction. Griffin & Ramberg (1976) investigated the vortex formation from a cylinder oscillating in line with flow when the natural vortex shedding frequency f_s matches with the cylinder oscillating frequency f_e. Ongoren & Rockwell (1988b) further studied the flow structure behind a cylinder oscillating at an angle of $0 \sim 90^o$ to the streamwise direction and identifies two basic modes: the symmetric and anti-symmetric modes, with the latter further divided into four sub-modes. Cetiner & Rockwell (2001) studied the lock-on state in the flow at $f_e/f_s = 0.5 \sim 3.0$ and found that the time-dependent transverse force is phase-locked to the cylinder motion and vortices are observed both upstream and downstream of the cylinder. Based on their experimental data, Xu *et al* (2006) observed a new mode at this flow condition, but at larger A/d (A being the oscillation amplitude; d being the cylinder diameter) or f_e/f_s, which consists of two rows of binary vortices symmetrically arranged about the centreline.

In terms of the experimental studies of vortex-induced vibration of two flexible cylinders in tandem arrangement, King (1977) investigated the wake interactions between two tandem flexible cylinders in a water flow and observed that vortex shedding patterns depend on the spacing between the cylinders. Tanida *et al* (1973) measured the lift and drag forces on the two cylinders when the downstream one oscillates streamwisely at $A/d = 0.14$ and $f_e/f_s = 0.5 \sim 2.2$. Okajima *et al* (2007) focused on the flow-induced vibration of two tandem cylinders and also showed different excitation regions determined by the reduced velocity and the spacing between the cylinders, L/d. In addition, Bearman (2011) provided useful reviews of some recent experimental works in this flow category together with some other recent works (Assi *et al*, 2010; Huera-Huarte & Bearman, 2011) focusing on the near wake interactions, although in these works the oscillation is induced by the flows rather than forced.

Previous investigations improved our understanding of flow around two in-line cylinders (oscillating or stationary). However, many aspects of this flow type remain unknown. For instance, to the best of the authors' knowledge, no study has been conducted so far regarding how a streamwisely forced oscillating cylinder affects a downstream cylinder. Yang *et al* (2014) recently addressed a similar tandem arrangement but the oscillation is in the transverse direction. This study aims for the dependence of the typical flow structures on A/d and f_e/f_s. The effects of L/d and Re are also examined. The results are further compared with stationary cylinder cases.

2 Experimental details

2.1 Flow visualization in a water tunnel

Laser-induced fluorescence (LIF) visualisations are carried out in a water tunnel with a working section of 0.15m×0.15m×0.5m. The working section is made of four 20mm thick perspex panels. The maximum velocity obtainable in the working section is 0.32m/s. Two acrylic circular tubes of identical diameter d =10mm are cantilever-mounted horizontally in a tandem manner at the mid-plane of the working section; see figure 1. The clearance between the cylinder ends and the tunnel wall is about 0.5mm. A DC motor is used to drive the upstream cylinder to oscillate harmonically at an amplitude of $A/d = 0.5$ in the streamwise direction. The oscillation frequency f_e varies from 0 to 9Hz which is well below the first-mode natural frequency of the fluid-cylinder system (estimated to be about 32Hz).

The cylinders have an aspect ratio of 15. King (1977) showed that for a stationary cylinder, an aspect ratio of 27 or larger is necessary to avoid the end effects.

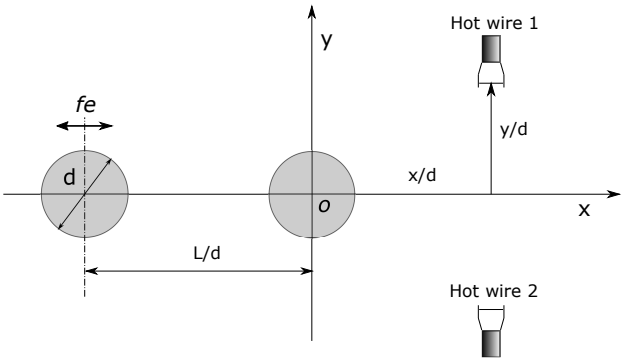

Fig. 1 Schematic arrangement of cylinders and two hot-wire probes; side view of the working section. The probes are placed at x/d = -1, 0, 1, 2, 5, 8 and y/d = 0, ±1, ±2, ±3, ±4, symmetrically about the centreline. The sketch is not to scale and the incoming flow is in the $+x$ direction.

However, for an oscillating cylinder this requirement is less stringent since the two-dimensionality will be enhanced by the vortex shedding from the oscillation motion. It has been observed that when the oscillation amplitude is greater than $0.02d$, the spanwise fluctuating pressure correlation coefficient ρ_p increases greatly, comparable to a stationary cylinder case, e.g. given a threshold $\rho_p = 0.5$, the spanwise correlation length is estimated to be $40d$, indicating a negligible end effect in the present experiments. Loosely speaking, the end surface of the oscillating cylinder can be considered as a small moving plate in the flow. A viscous transverse wave forms in the Stokes layer (the boundary layer at the cylinder end Wu *et al* 2006) and propagates away from the cylinder. The wave keeps the fluid away from the cylinder and the end effect is weakened.

Rhodamine Dye (6G 99%) is introduced through one injection pinhole located at the mid-span of the cylinders at the top and the bottom surface. A Spectra-Physics Stabilite 2017 Argon ion laser with a maximum power output of 4W is used for illumination. Images are taken by a digital video camcorder (JVC GY-DV500E) at a framing rate of 25Hz. Measurements are carried out for cylinder spacing L/d = 2.5, 3.5, 4.5 and Re based on cylinder diameter 150 ∼ 1000.

2.2 Quantitative measurements in a wind tunnel

The wind tunnel is described in details in Zhou *et al* (2002), which has a working section of 2.4×0.6×0.6m. The maximum wind speed in the working section is 50m/s. Two aluminium alloy cylinders of d = 15mm with an aspect ratio 23 are cantilever-supported in the horizontal mid-plane of the working section. Their spacing can be adjusted from L/d = 2.5 to 4.5; see figure 1. One microcomputer-controlled DC motor system is used to drive the upstream cylinder to oscillate harmonically at A/d = 0.67, and $f_e = 0 \sim 20$Hz which is well below the first-mode natural frequency of each cylinder (≈272 Hz). The free stream turbulence intensity is measured to be 0.4%. Most measurements are conducted at free stream velocity U_∞ = 1.0 m/s giving a Re = 1150. At this speed, the vortex shedding frequency from the upstream cylinder is locked on to the cylinder motion. It must be noted that in order to account for the low frequency unsteadiness at this low free stream velocity, three additional screen layers are installed at the contraction section and the operation steadiness is verified by a hot-wire measurement test. All the hot-wire data are also high-pass filtered in order to further remove any possibly remaining low frequency unsteadiness and to increase the signal-noise ratio.

The dominant frequencies in the flow are measured using two hot-wire probes, placed at locations shown in figure 1. The sampling frequency is 1.5kHz per channel and the typical duration of each record is about 30s. The hot-wires are calibrated over the range of 0.3 ∼ 10m/s using TSI-1128 velocity calibrator.

3 Typical flow structures

In this article, two dimensionless frequencies are used. The first accounts for the forcing frequency, namely f_e/f_s, where f_e is the cylinder oscillation frequency and f_s is the vortex shedding frequency from an isolated stationary cylinder. In water tunnel visualisations, $f_s = 0.3 \sim 2$Hz while in wind tunnel measurements f_s = 13.3Hz. Note that f_s is not the vortex shedding frequency of two stationary tandem cylinders since it depends not only on Re but also on the spacing L/d. The second is $f^* = fd/U_\infty$, which is used to quantify the characteristic frequency in the power spectrum measurements.

From the flow visualisation, it is found that the flow structure around the two cylinders largely depends on the combination of f_e/f_s and A/d for $L/d = 2.5 \sim 4.5$, similarly to the one for a single isolated oscillating cylinder (Karniadakis & Triantafyllou, 1989; Xu *et al*, 2006). This suggests the dominance of the oscillating cylinder's wake over the downstream stationary one's. Three distinguishable flow patterns can be identified when the vortex shedding frequency is locked on to f_e, with the first two patterns (SA and AA mode) showing new vortex structures which have never been observed and the third pattern (A mode) similar to a previous reported one.

3.1 Symmetric-antisymmetric binary street (SA-mode)

For $f_e/f_s \geq 1.6$ and $A/d = 0.5$, the flow behind the downstream cylinder is characterised by a binary street that consists of two outer rows (towards the free stream region) of symmetrically arranged vortices originated from the oscillating cylinder and two inner rows (closed to the centreline) of anti-symmetrically arranged vortices generated by the downstream cylinder; see figure 2.

Each pair shed from the upstream cylinder further comprises a pair of counter-rotating vortical structures, which is similar to the 2P mode in Williamson & Roshko (1988) but with a significant difference, i.e. they are mirror imaged about the centreline, instead of alternative. To label the difference, we name it a binary vortex structure. A better understanding of the formation of this structure is via sequential photographs at various phases within one typical period of the cylinder oscillation. When the oscillating cylinder moves upstream (from $+A$ to $-A$, figure 2 a-c), one clockwisely rotating structure Au1 forms due to the natural vortex shedding. As it moves downstream (from $-A$ to $+A$ c-f), fluid close to the cylinder wall moves along due to viscous effect, while fluid further away moves upstream relatively to it. Since the velocity maxima of the cylinder is 3.77cm/s ($U_m = 2\pi A f_e$, $f_e = 1.2$Hz) and U_∞=2.7cm/s, the maximum relative velocity is 1.07 cm/s, resulting in an instantaneous relative Re= 120 based on this relative velocity, which exceeds the critical Re$\approx$ 40 (see Schlichting & Gersten, 2000) and Au2 begins to form in an anti-clockwise sense. Eventually, the structure containing the pair Au1 and Au2 separates from the cylinder (f-h) and is swept downstream by U_∞. A similar flow structure can be observed at a higher Re = 500 (not shown).

Figure 3 shows the power spectral density function E_u of the measured hot-wire signals above the centreline. Between the two cylinders at $x/d = -1$ (figure 3a), E_u exhibits one pronounced peak at $f = f_e$ along the y direction, indicating the lock-on event between the binary vortex shedding and the cylinder oscillation motion. The peak corresponds to $f^* = 0.29$. The spectral phase (not shown) measured from the two hot-wire probes arranged symmetrically about $y = 0$ is zero at this peak, reassuring the symmetry arrangement of the binary vortices (figure 2). At $y/d > 1$, another peak occurs at $f = 2f_e$ ($f^* = 0.58$) and becomes more pronounced when y/d increases, which apparently indicates the vortex pair in each binary vortex (figure 2).

Behind the downstream cylinder at $x/d = 2$, one strong peak appears at $f = 0.5f_e$ for $y/d \leq 1$ only (figure 3b). This peak is ascribed to the two inner rows of

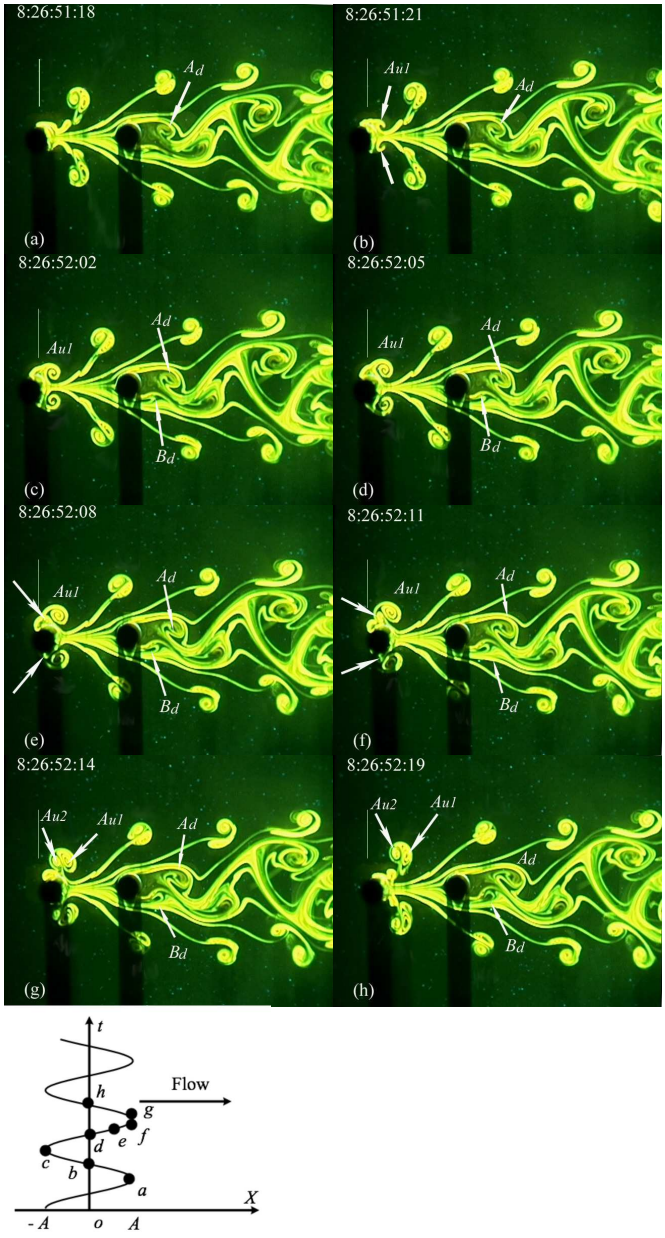

Fig. 2 Sequential photographs of a symmetric-antisymmetric binary street (SA-mode) at $f_e/f_s = 1.8$. $L/d = 3.5$, Re = 300, $A/d = 0.5$. The phase of each photo is indicated in the side plot, where t and X represent time and the streamwise displacement, from the reference position (X = 0) of the upstream cylinder, respectively. The reference position is marked by a vertical line near the upstream cylinder in the photographs.

vortices shed from the downstream cylinder. It is further corroborated by a spectral phase near π at $f/f_e = 0.5$ (not shown) between the two hot-wire measurements mentioned above, which is in consistence with the anti-symmetric shedding manner shown in figures 2. It indicates that the vortex shedding frequency of the downstream stationary cylinder halves that of the bi-

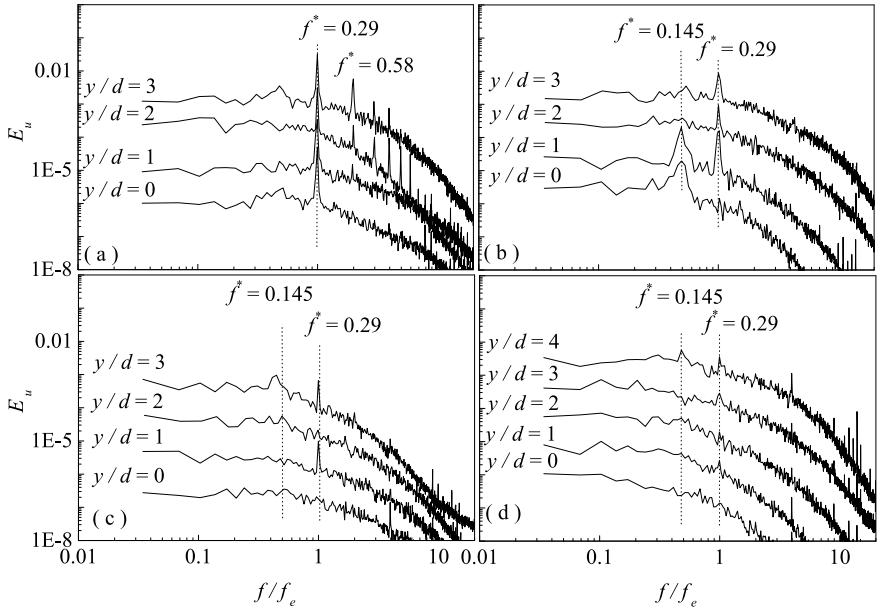

Fig. 3 Power spectral density function of the hot-wire signals for the SA-mode at $f_e/f_s = 1.45$, $A/d = 0.67$, $L/d = 3.5$ and Re = 1150. (a) x/d = -1; (b) $x/d = 2$; (c) $x/d = 5$; (d) $x/d = 8$; refer to figure 1 for locations. Spectral lines are shifted in the vertical direction for clearer presentation purposes.

nary vortices. For $y/d \geq 2$, the peak at $0.5f_e$ disappears but the one at f_e remains visible, in line with the observation that the symmetrically arranged binary vortices occur fairly far away from the centreline. The peak at $f = 2f_e$ or $f^* = 0.58$ in figure 3 (a) is not seen at $x/d = 2$, suggesting that one of the counter-rotating vortical structures has vanished due to vorticity cancellation.

Further downstream at $x/d = 5$ (figure 3c), on the one hand, the peak at $f = 0.5f_e$ disappears completely, indicating the disappearance of the alternating inner vortex street generated by the downstream stationary cylinder; on the other hand, the peak at $f = f_e$ is still discernible, referring to a longer persistence of the binary vortices, i.e. the vorticity concentration of the vortical structures separated from the upstream cylinder are significantly stronger, therefore survive for longer time.

Both inner and outer vortex streets decay fast. By $x = 8d$, all peaks are barely visible. Zhou *et al* (2002) observed a faster decay of two coupled streets generated by two side-by-side cylinders, compared to the street behind an isolated fixed cylinder, and attributed it to the strong vortex interaction between the inner and outer rows. This mechanism is probably also responsible for the observation in this experiment. The vorticity cancellation between the opposite-sensed rotating structures in the binary vortex may further accelerate the decay of these vortex streets.

In order to have a better understanding about why the binary vortex frequency doubles the one of the alternative shedding from the downstream cylinder, a hot-wire measurement is conducted for the case where the upstream cylinder is stationary and the results are shown in figure 4. E_u displays only one peak at $f^* = 0.127$ at both x/d locations which reflects that both cylinders generate vortices at the same pace (Igarashi, 1981). Evidently, the cylinder oscillation has changed the vortex shedding frequency from f^*= 0.127 to 0.29 for the upstream cylinder and to 0.145 for the downstream cylinder. It seems plausible that flow separation from the upstream cylinder may trigger the one from the downstream cylinder or vice versa, implying that the two frequency must be identical. As a result, the symmetric vortex shedding frequency from the upstream cylinder must double the one from the downstream cylinder since the latter is alternative. Whereas if the vortex shedding modes of both cylinders are the same, either symmetric or anti-symmetric, their shedding frequency must also be identical, just like the case of two stationary cylinders (Ishigai *et al*, 1972). The assertion is further confirmed by the flow structures of the other two modes; see § 3.2 and § 3.3 below.

E_u with and without the oscillation are compared in figure 5 for a better understanding of the influence of the upstream cylinder's oscillation motion on the downstream one. When the oscillation occurs, the peak appears at $f = 0.5f_e$ with a magnitude about 0.002; in contrast, the magnitude of the peak for a stationary

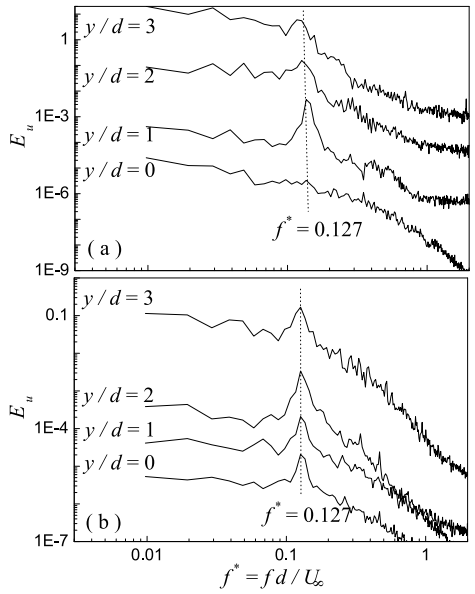

Fig. 4 Power spectral density function of hot-wire signals for the case where the upstream cylinder is stationary, i.e. $f_e/f_s = 0$: (a) $x/d = -1$, between the cylinders; (b) $x/d = 2$, behind the downstream cylinder. $L/d = 3.5$, and Re = 1150. Spectral lines are shifted in the vertical direction.

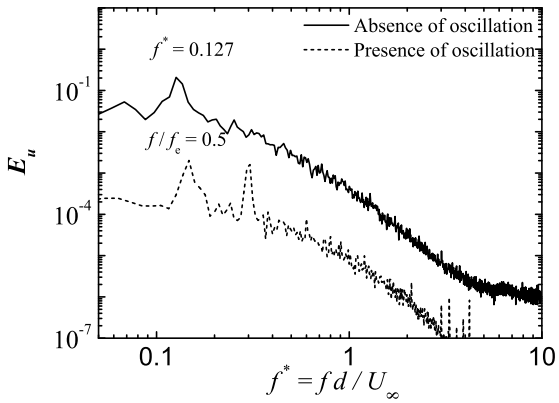

Fig. 5 Power spectral density functions of the hot-wire signals with and without the oscillation of the upstream cylinder. $L/d = 3.5$, Re = 1150. The upstream cylinder's oscillation condition is $f_e/f_s = 1.45$, $A/d = 0.67$. The measurement location is at $x/d = 2$ and $y/d = 1$, which is in the pathway of the inner vortex street behind the downstream cylinder.

case is about two orders of magnitude larger (≈ 0.207), demonstrating a great loss of the vortex strength under the influence of the symmetrical binary vortices.

3.2 Antisymmetric-antisymmetric binary street (AA-mode)

When f_e/f_s reduces to $1.0 \sim 1.6$ and A/d remains at 0.5, a completely different flow structure emerges; see figure 6. A careful examination of the video reveals that a binary street occurs in the flow field, which consists of two outer rows of binary vortices such as Au and Bu, originated from the upstream cylinder (also different to the 2P mode in Williamson & Roshko 1988), and two inner rows of single vortices, denoted by Ad and Bd, generated by the downstream cylinder (similar to the 2S mode). The two successive vortices alternately shed from the upstream cylinder quickly move to one side of the centreline before reaching the downstream cylinder. The structure Au2, which is originated from the upper side of the upstream cylinder, crosses the centreline to approach Au1 originated from the lower side of the same cylinder (figure 6a). The two vortices eventually pair up and form a binary vortex in the outer row (b-d). But Au2 appears to be losing its identity quickly due to vorticity cancellation by Au1, leaving a single vortex Au remaining (e-h). The evolution of vortices Bu1 and Bu2, which are shed from the upper and lower side of the upstream cylinders respectively, is quite similar to that of Au1 and Au2, although they end up above the centreline.

The motion of the upstream cylinder plays a key role to induce a vortex across the centreline which then merges with the one on the other side. Note that the vortex shedding frequency from the upstream cylinder is locked to f_e, i.e. each time when the cylinder moves against U_∞, one vortex forms, e.g. the vortex Cu2 in figure 6(e) is just born. The movement in the upstream direction reduces the backpressure on the cylinder. The very low pressure in the lower region draws Cu2 towards the centreline (f), which then is pushed downstream by the ensuing streamwise movement (g-h).

Figure 7 (a) shows declined spectra E_u as y/d increases. Another peak occurs at $f = 0.5f_e$ for $y/d \geq 1$ and $x/d = -1$, which is significantly more pronounced than that at $f = f_e$. The former corresponds to the observation in figure 6 that every other vortex (e.g. Au2 or Bu2) shed from the upstream cylinder cross the centreline to coalesce with a cross-stream vortex.

At $x/d = 2$, the peak at $f = 0.5f_e$ remains pronounced and the one at $f = f_e$ can also be seen, albeit much weaker. The latter, particularly at small y/d, is believed to be attributed to the vortex shedding from the downstream cylinder. This is supported by our PIV measurements (not shown) that the vortices shed from the downstream cylinder display a weaker intensity compared with those originated from the upstream cylinder; it is consistent with the proposition that the frequency of the vortex shedding from the two cylinders should be identical given the same shedding mode. Both peaks are identifiable at $x/d = 5$ and 8 (7c and d), suggesting a longer survival of the binary street than at $f = 1.0f_e$.

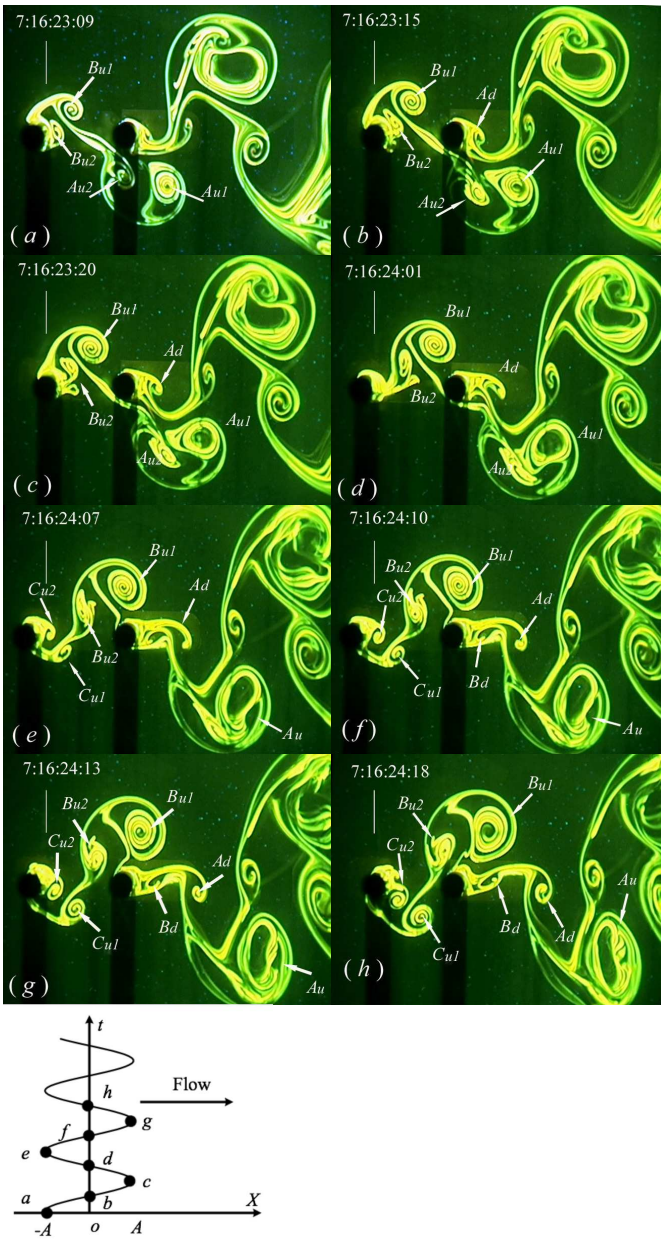

Fig. 6 Sequential photographs of an antisymmetric-antisymmetric binary street (AA-mode) at $f_e/f_s = 1.08$. $L/d = 3.5$, Re = 300, $A/d = 0.5$.

3.3 Antisymmetric single street (A-mode)

The flow of this mode is characterised by a single staggered street, behind both cylinders, for $0.5 < f_e/f_s \leq 1.0$ and $A/d = 0.5$. Although the shedding pattern can be categorised as the 2S mode (Williamson & Roshko, 1988), here we adopt a different terminology as A-mode to be consistent with the previous two modes. Figure 8 presents sequential photographs of this case. It can be seen that under the influence of the downstream stationary cylinder, vortices Au and Bu are separated alternately to the upper and lower sides of the centreline. These vortices merge to the surrounding shear layers, separate from the downstream cylinder and form a staggered vortex street downstream. Apparently the vortex shedding frequency must be identical between the upstream and the downstream cylinder, which is also locked-on to the cylinder oscillation. This is confirmed by the power spectra in figure 9, which exhibits a single peak at $f = f_e$ for all x.

4 Discussion

4.1 The effect of L/d and Re on the flow structure

Figure 10 shows the dependence of the flow structure on the spacing of the two cylinders. As can been observed, the typical flow structures (SA-mode) are essentially the same regardless of the L/d value within the testing range. In contrast, the flow behind two tandem stationary circular cylinders does depend on L/d, which can be classified into three flow regimes as shown in Igarashi (1981) and Zdravkovich (1987).

The degree of the Re dependence is examined in figure 11. When undergoing oscillation, Re does not seem to affect the vortex shedding mode to a significant extent although the flow becomes turbulent at higher Re. The same mode can be observed as Re increases from 300 to 800. Nevertheless, Re is an important influential factor for single cylinder case (Gerrard, 1978) and two stationary tandem cylinder case (Ljungkrona *et al*, 1991). Our measurements at the fixed $A/d = 0.5$ indicates a negligible Re effect on the critical f_e/f_s ratio, where the flow pattern changes from one mode to another, for Re > 300. It thus can be deduced that it is the oscillation of the upstream cylinder which determines different flow patterns, the influence of Re and L/d is rather weak in comparison.

4.2 Theoretical consideration of the SA-mode occurrence

The flow between the cylinders displays a remarkable symmetric binary vortex street pattern in this mode, which is quite similar to the S-II mode previously reported in Xu *et al* (2006), which was found that the vorticity produced by the streamwisely oscillating cylinder surface consists of two components: one is identical to that generated by a stationary cylinder subjected to a steady uniform cross flow; the other depends on the cylinder oscillation, anti-symmetric or symmetric about the centreline. The non-linear interaction between the two components results in various flow modes.

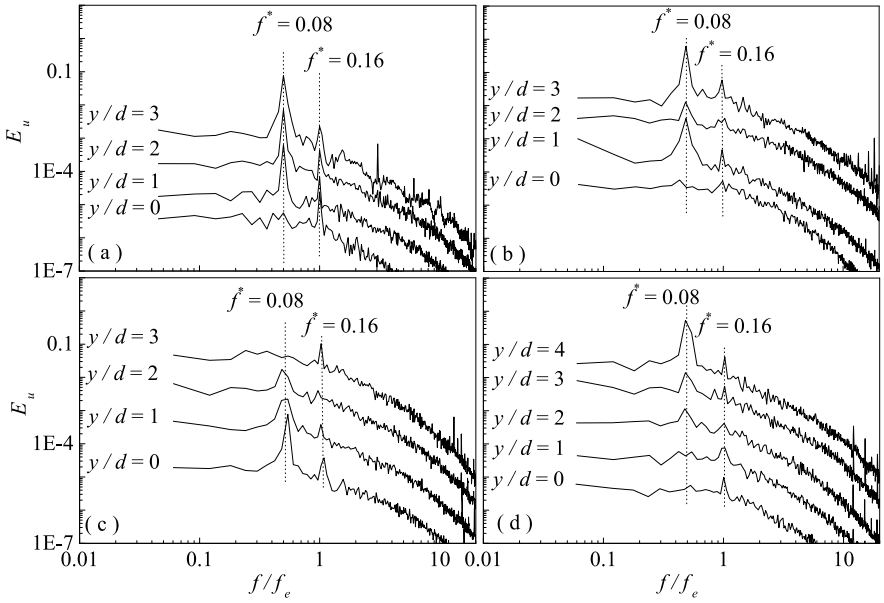

Fig. 7 Power spectral density function of hot-wire signals for the AA-mode at $f_e/f_s = 0.8$, $A/d = 0.67$, $L/d = 3.5$ and Re = 1150. (a) $x/d = -1$; (b) $x/d = 2$; (c) $x/d = 5$; (d) $x/d = 8$. Spectral lines are shifted in the vertical direction for clearer presentation purposes.

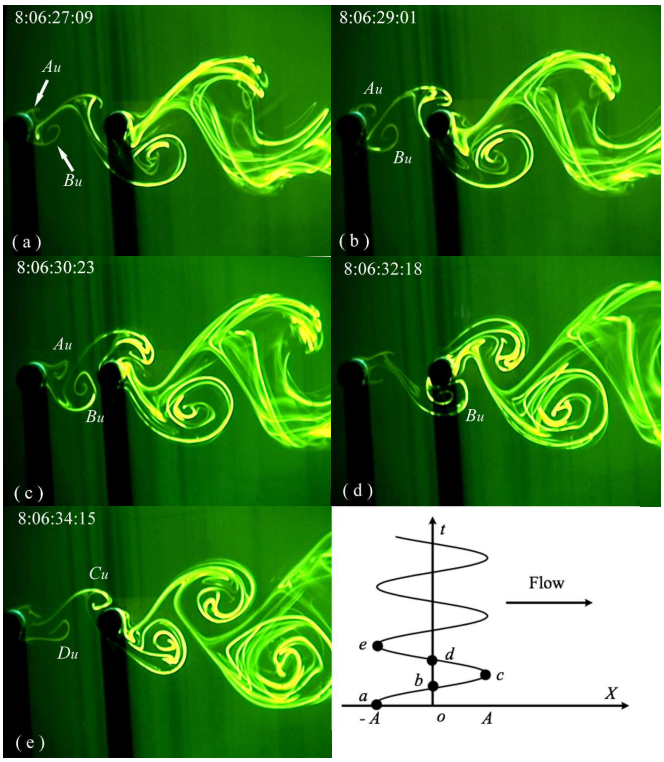

Fig. 8 Sequential photographs of an antisymmetric single street (A-mode) at $f_e/f_s = 0.5$. $L/d = 3.5$, Re = 150, $A/d = 0.5$.

It is demonstrated in Xu *et al* (2006) that for a cylinder oscillating at an amplitude

$$X(t) = A\cos(2\pi f_e t + \psi_o), \tag{1}$$

f_e being the frequency and ψ_o being the initial phase angle, the two dimensional vorticity equation, when applied on the surface of the cylinder, can be written as

$$\frac{\partial \omega_z}{\partial t} = \frac{8\pi^2 f_e^2 A}{d}\cos(2\pi f_e t + \psi_o)\sin\theta, \tag{2}$$

where θ is the azimuthal component of the cylindrical coordinates. Integrating yields the vorticity created on the surface

$$\omega_z = \frac{4\pi f_e A}{d}\sin(2\pi f_e t + \psi_o)\sin\theta + \omega_{z,c}(\theta, p) \tag{3}$$

$$= \omega_{z,u}(\theta, t) + \omega_{z,c}(\theta, p), \tag{4}$$

where $\omega_{z,u}(\theta, t)$ is the oscillation-induced vorticity, which is anti-symmetric about the centreline, but symmetric in terms of magnitude; $\omega_{z,c}(\theta, p)$ is an oscillation-independent component, which is the vorticity associated with two stationary cylinders in a steady uniform flow, i.e. $\omega_z(\theta, t) \equiv 0$. If $f_e A$ is large enough, $\omega_{z,c}(\theta, p)$ can be neglected compared to $\omega_{z,u}(\theta, t)$ and the vorticity generated by the upstream cylinder is governed by the oscillation motion and is symmetric about the centreline in terms of magnitude, producing the SA-mode. Note that vortex shedding from the downstream cylinder is always alternative, which is not affected by the flow structure between the cylinders.

The occurrence of the SA-mode may also be inferred in terms of the vorticity flux σ on the surface of a cylinder as suggested in Morton (1984) and Blackburn & Henderson (1999)

$$\sigma = -\nu \mathbf{r}_o \cdot \nabla\omega_z = -\mathbf{r}_o \times (\nabla p + \mathbf{a}) - \frac{1}{\rho r}\frac{\partial p}{\partial \theta} \tag{5}$$

$$+4\pi^2 f_e^2 A\cos(2\pi f_e t + \psi_o)\sin\theta |r| \mathbf{r}_o,$$

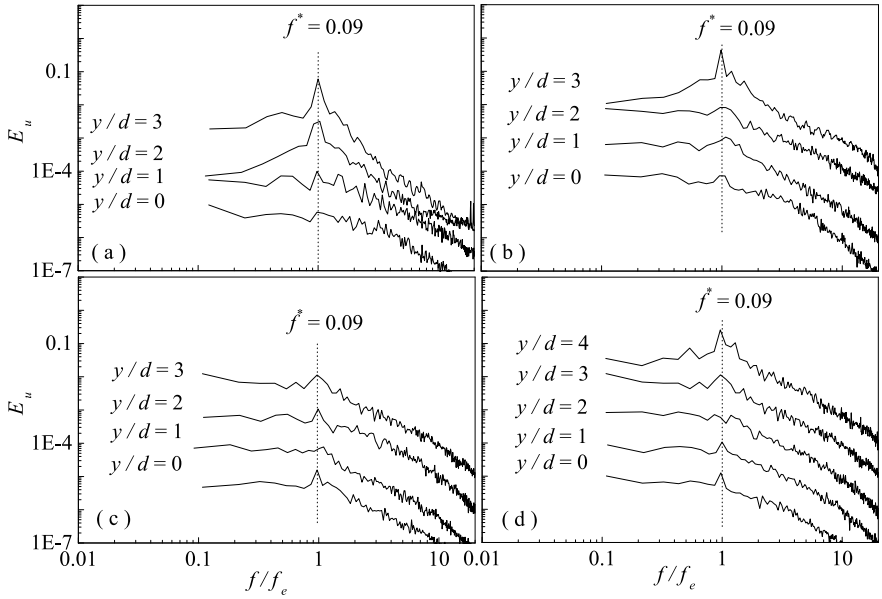

Fig. 9 Power spectral density function of hot-wire signals for the A-mode at $f_e/f_s = 0.45$, $A/d = 0.67$, $L/d = 3.5$ and Re = 1150. (a) $x/d = -1$; (b) $x/d = 2$; (c) $x/d = 5$; (d) $x/d = 8$.

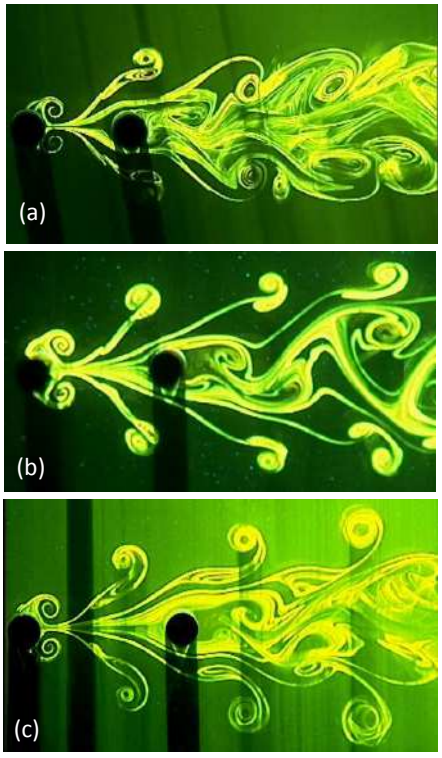

Fig. 10 Flow structure at various L/d. Re = 300, $f_e/f_s = 1.8$, $A/d = 0.5$. (a) $L/d = 2.5$; (b) $L/d = 3.5$; (c) $L/d = 4.5$

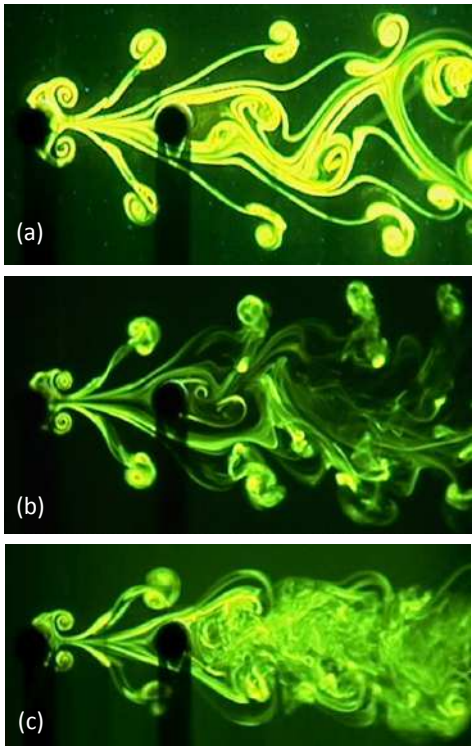

Fig. 11 Flow structure at various Re. $L/d = 3.5$, $f_e/f_s = 1.8$. (a) Re=300; (b) Re=500; (c) Re=800.

where $\mathbf{r}_o$ is the unit vector in the radial direction; σ represents the vortex flux strength per unit time and area on a cylinder surface. Equation (6) comprises of two components: the tangent gradient of the pressure p and the tangent component of the acceleration. The first component does not depend on oscillation but the second one does. If $f_e A$ is large enough, σ will be symmetric about the centreline.

Defining a relative Reynolds number based on the cylinder's relative velocity to the free stream U_∞, when the cylinder moves upstream, $\Delta U = U_\infty - \dot{X} = U_\infty +$

$2\pi f_e A$ and ΔRe always exceeds the critical Re for the formation and separation of vortices in an isolated cylinder case, which is about 50. However, when the cylinder moves downstream, $\Delta U = U_\infty - 2\pi f_e A$. If the maximum $\dot{X}$ exceeds U_∞, i.e. $2\pi f_e A > U_\infty$, ΔU is negative relative to U_∞. The condition for the occurrence of the SA-mode may start, given ΔU negative and sufficiently large in magnitude, as

$$\Delta\mathrm{Re} = \frac{(2\pi \mathrm{f_e A} - \mathrm{U_\infty})\,\mathrm{d}}{\nu} \geq \Delta\mathrm{Re_c}, \tag{6}$$

where $\Delta\mathrm{Re_c}$ is a critical Reynolds number, which is suggested to be less than 5 for a single streamwise oscillating cylinder case (Xu *et al*, 2006). Solving (6) in terms of f_e/f_s, A/d and Strouhal number St, we obtain

$$f_e/f_s \geq \frac{(1 + \Delta\mathrm{Re_c}/\mathrm{Re})}{2\pi \mathrm{St}\,(\mathrm{Re})} \left(\frac{A}{d}\right)^{-1} = (f_e/f_s)_c\,, \tag{7}$$

where St=St(Re) is for an isolated stationary cylinder wake and is well documented in Chen (1987) and Blevins (1994) for example; $(f_e/f_s)_c$ is the threshold value for the occurrence of the SA-mode. Based on (7), $(f_e/f_s)_c$ is inversely proportional to A/d. If (7) is not satisfied, e.g. in cases of a small ΔU, $\Delta\mathrm{Re} < \Delta\mathrm{Re_c}$, then A- or AA-mode occurs.

At Re$>$ 300, St(Re)$\approx$0.2, $\Delta\mathrm{Re_c}/\Delta\mathrm{Re} \approx 0$ (given $\Delta\mathrm{Re_c} \approx$5), the Re effect on the generation of the SA mode should be negligible. Equation (7) can then be simplified as

$$f_e/f_s \geq (f_e/f_s)_c \approx \frac{5}{2\pi}\left(\frac{A}{d}\right)^{-1}. \tag{8}$$

This relation gives rise to the curve $(f_e/f_s)_c = 0.8\,(A/d)^{-1}$ in figure 12, which is used to predict the occurrence of the SA-mode. It is worth pointing out that $\Delta\mathrm{Re_c}$ could be slightly different from 5 in the presence of a downstream cylinder, which depends on L/d, albeit weak as suggested in figure 10.

5 Conclusion

This article presents wake patterns excited by the streamwise oscillation of the upstream cylinder. Three distinguishably different patterns, as summarised in figure 13, are governed primarily by the oscillation frequency f_e/f_s and the amplitude A/d, weakly by the cylinder spacing L/d and Re. The SA-mode occurs for $f_e/f_s > (f_e/f_s)_c$ (about 1.45 for $A/d = 0.67$, 1.6 for $A/d = 0.5$). The upstream oscillating cylinder generates binary vortices symmetrically arranged about the centreline, each binary vortex consisting of a pair of counter-rotating vortices. Meanwhile, the downstream cylinder sheds vortices alternately at a frequency of

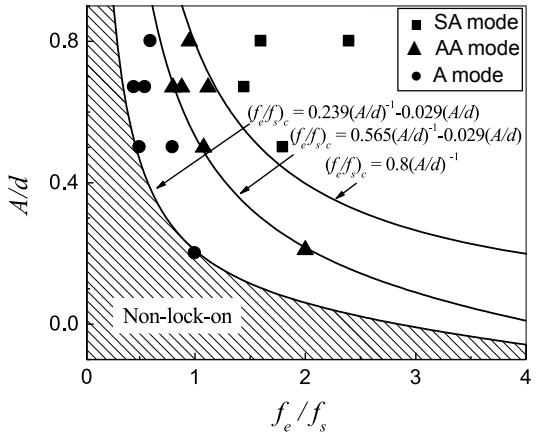

Fig. 12 Dependence of the flow structure on A/d and f_e/f_s. The curve $(f_e/f_s)_c = 0.8(A/d)^{-1}$ indicates the critical f_e/f_s for the occurrence of the SA mode; $(f_e/f_s)_c = 0.565(A/d)^{-1} - 0.029(A/d)$ separates the A and AA modes; $(f_e/f_s)_c = 0.239(A/d)^{-1} - 0.029(A/d)$ separates the lock-on and non-lock-on states.

one half of the oscillation frequency. A complex vortex street occurs behind the downstream cylinder, which includes two outer rows of symmetrically arranged binary vortices originating from the upstream oscillating cylinder and two inner rows of staggered vortices generated by the downstream stationary cylinder. Analysis has been developed to predict the occurrence of the SA-mode flow structure, which is in good agreement with the experimental data. The AA-mode occurs for $0.7 \sim 2.4 \leq f_e/f_s \leq (f_e/f_s)_c$, when alternate vortex shedding occurs for both cylinders. The flow behind the downstream cylinder is characterised by a complex vortex street that consists of two outer rows of binary vortices, originated from the upstream cylinder, and two inner rows of single vortices shed from the downstream cylinder. The vortices in the two outer or two inner rows are spatially antisymmetrical about the centreline. The A-mode emerges behind the downstream cylinder at $0.27 \sim 0.61 \leq fe/fs \leq 0.7 \sim 1.6$. In general, f_e/f_s, at which a particular mode of the flow structure occurs, decreases as A/d increases.

In general, at a fixed A/d, the frequency f space is divided into three ranges, each corresponds to one mode, i.e. $f(A) < f(AA) < f(SA)$. It is found, from a quick comparison of the three patterns (e.g. figure 2, 6 and 8 and the corresponding PSD for $x/d > 0$), that the widest wake behind the downstream cylinder is observed when f_e/f_s is near unity. If we consider the two-cylinder as a system, it implies that f_s is also in the vicinity of the nature frequency of the entire system, the interaction of the two cylinders leads to a resonant effect, which outputs the most energetic wake. Consider a small fluid parcel with a mass m, its displacement in

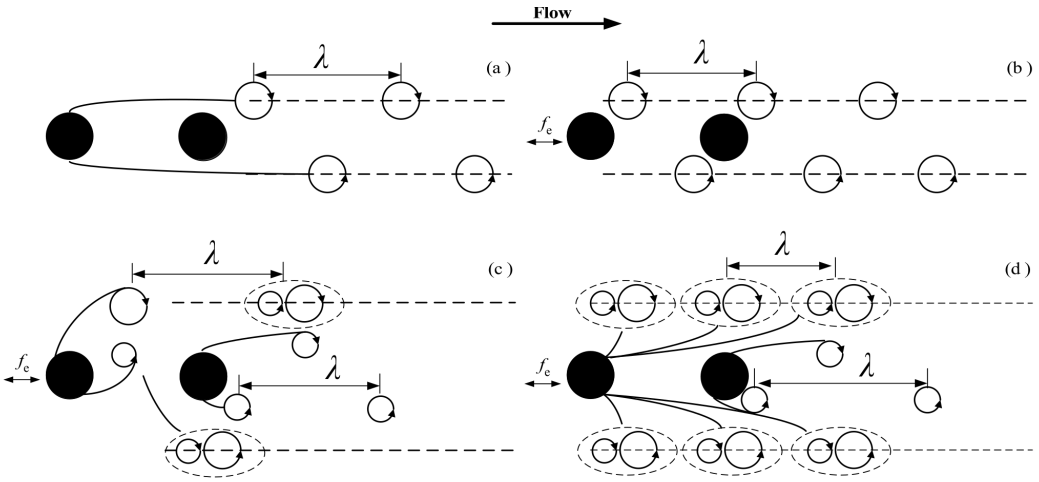

Fig. 13 Summary sketch of dominant flow structures (λ represents the vortex wavelength). (a) Two inline stationary cylinders; (b) A-mode; (c) AA-mode; (d) SA-mode

the y direction is $Y(t)$, which is a function of time and similar to a simple harmonic motion. $Y(t)$ can be described by a linear system:

$$m\ddot{Y}(t) + c\dot{Y}(t) + kY(t) = \mathcal{F}, \tag{9}$$

where the input $\mathcal{F}$, at a fixed Re, is a function of f_s, A and d, i.e. $\mathcal{F} = \mathcal{F}(f_s, A, d)$. This system has a natural frequency $f_o = \sqrt{(1-\zeta^2)(k/m)}$, with the damping ratio ζ, which is of an isolated cylinder. It implies that if f_e is set near f_o, the resonance effect is seen, which is verified by figure 6. This observation shows that a properly chosen streamwise oscillation frequency of one component is able to induce a resonant effect of the entire system, which can maximise the spanwise mixing in the far wake region.

Acknowledgements The authors would like to thank the funding support by NSFC through grant 11472158, United Kingdom Royal Society of Engineering Newton Research Collaboration Fund (RAE NRCP/1415/130).

References

Assi, G.R.S., Bearman, P.W. & Meneghini, J., 2010 On the wake-induced vibration of tandem circular cylinders: the vortex interaction excitation mechanism. *J. Fluid Mech.* **661**, 365–401

Bearman, P.W. 2011 Circular cylinder wakes and vortex-induced vibrations. *J. Fluid Struct.* **27**, 648–658

Blackburn H. M. & Henderson R. D. 1999 A study of two-dimensional flow past an oscillating cylinder. *J. Fluid Mech.* **385**, 255–286

Blevins, D. 1994 Flow-induced vibration *Krieger Publishing Company* Florida, pp48

Carberry, J., Sheridan, J. & Rockwell, D. 2001 Forces and wake modes of an oscillating cylinder. *J. Fluid Struct.* **15**, 523–532

Cetiner, O. & Rockwell, D. 2001 Streamwise oscillations of a cylinder in a steady current (Part I, Locked-on states of vortex formation and loading; Part II, Free-surface effects on vortex formation and loading). *J. Fluid Mech.* **427**, 1–59

Chen, S. S. 1987 Flow-induced Vibration of Circular Cylinder Structures *Hemisphere Publishing Corporation* pp260

Gerrard, J. K. 1978 The wakes of cylindrical bluff bodies at low Reynolds number. *Philos. T. R. Soc. A* **288**, 351–382

Griffin, O. M. & Ramberg, S. E. 1976 Vortex shedding from a cylinder vibrating in line with an incident uniform. *J. Fluid Mech.* **75**, 257–271

Hardin, C. J. & Wang, Y. F. 2003 Sound generation by aircraft wake vortices *NASA/CR-2003-0212674*

Hover, F. S., Techet, A. H. & Triantafyllou, M. S. 1998 Forces on oscillating uniform and tapered cylinders in crossflow. *J. Fluid Mech.* **363**, 97–114

Huera-Huarte, F.J. & Bearman, P.W., 2011 Vortex and wake-induced vibrations of a tandem arrangement of two flexible circular cylinders with near wake interference. *J. Fluid Struct.* **27**, 193–211

Igarashi, T. 1981 Characteristics of the flow around two circular cylinders arrangement in tandem (1st report). *Bulletin of the JSME* **24** (188), 323–331

Inoue, O. & Hatakeyama, N. 2002 Sound generation by a two-dimensional circular cylinder in a uniform flow. *J. Fluid Mech.* **471**, 285–314

Ishigai, S., Nishikawa, E., Nishmura, K. & Cho, K. 1972 Experimental study on structure of gas flow in tube banks with tube axes normal to flow (Part

1, Karman vortex flow around two tubes at various spacings). *Bulletin of the JSME* **15**, 949–956

Karniadakis, G. E. & Triantafyllou, G. 1989 Frequency selection and asymptotic states in laminar wakes. *J. Fluid Mech.* **199**, 441–469

King, R. 1977 A review of vortex shedding research and its application. *Ocean Eng.* **4**, 141–171

Ljungkrona, L., Norberg, Ch. & Sunden B. 1991 Free-stream turbulence and tube spacing effects on surface pressure fluctuations for two tubes in an in-line arrangement. *J. Fluid Struct.* **5**, 701–727

Ming, X. & Gu, Y.S. 2005 Flow control and mechanism for slender body at high angle of attack. *Mod. Phys. Lett. B* **19**, 1571–1574

Morton B. R. 1984 The generation and decay of vorticity. *Geophys. Astrophys. Fluid Dyn.* **28**, 277–308

Okajima, A., Yasui, S., Kiwata, T., & Kimura, S. 2007 Flow-induced streamwise oscillation of two circular cylinders in tandem arrangement. *Int. J. Heat Fluid Fl.* **28**(4), 552–560

Ongoren, A. & Rockwell, D. 1988b Flow structure from an oscillating cylinder. Part II. Mode competition in the near wake. *J. Fluid Mech.* **191**, 225–245

Schlichting, H. & Gersten, K. 2000 Boundary layer theory, 8th revised and enlarge edition *Springer-Verlag Berlin Heidelberg*, pp22

Staubli, T. & Rockwell, D. 1989 Pressure fluctuations on an oscillating trailing edge. *J. Fluid Mech.* **203**, 307–346

Sumner, D. 2010 Two circular cylinders in cross-flow: A review. *J. Fluid Struct.* **26**(6), 849–899

Tanida, Y., Okajima, A. & Watanabe Y. 1973 Stability of a circular cylinder oscillating in a uniform flow or in a wake. *J. Fluid Mech.* **61**, 769–784

Williamson, C. H. K. & Roshko, A. 1988 Vortex formation in the wake of an oscillating cylinder. *J. Fluid Struct.* **2**, 355–381

Wu J.Z., Ma H.Y. & Zhou M.D. 2006 Vorticity and Vortex Dynamics *Springer* USA, pp150–160

Xu, S. J. & Zhou, Y. 2003 Reynolds number effects on the flow structure behind two side-by-side cylinders. *Phys. Fluids* **15**, 1214–1219

Xu, G & Zhou, Y 2004 Strouhal numbers in the wake of two inline cylinders. *Exp. Fluids* **37**, 248–256

Xu, S. J., Zhou, Y. & Wang, M. H. 2006 A symmetric binary vortex street behind a longitudinally oscillating cylinder. *J. Fluid Mech.* **556**, 27–43

Yang, Y., Aydin, T. B., & Ekmekci, A. 2014 Flow past tandem cylinders under forced vibration. *J. Fluid Struct.* **44**, 292–309

Zdravkovich, M. M. 1987 The effects of interference between circular cylinders in cross flow. *J. Fluid Struct.* **1**, 239–261

Zhou, Y., Wang, Z. J., Xu, S.J. & Jin, W. 2001 Free vibrations of two side-by-side cylinders in a cross flow. *J. Fluid Mech.* **443**, 197–229

Zhou, Y., Zhang, H. J. & Yiu, M.W. 2002 The turbulent wake of two side-by-side circular cylinders. *J. Fluid Mech.* **458**, 303–332